International Journal of Rock Mechanics & Mining Sciences 52 (2012) 9–17

Contents lists available at SciVerse ScienceDirect

International Journal of Rock Mechanics & Mining Sciences

journal homepage: www.elsevier.com/locate/ijrmms

Sliding crack model for nonlinearity and hysteresis in the uniaxial stress–strain curve of rock

E.C. David [a,*], N. Brantut [b], A. Schubnel [b], R.W. Zimmerman [a]

[a] Department of Earth Science and Engineering, Imperial College, London, UK
[b] Laboratoire de Géologie, CNRS UMR 8538, École Normale Supérieure, Paris, France

ARTICLE INFO

Article history:
Received 24 September 2009
Received in revised form
30 January 2012
Accepted 2 February 2012

Keywords:
Cracks
Sliding cracks
Hysteresis
Uniaxial compression
Sandstone
Granite

ABSTRACT

Uniaxial compression tests on rocks, if conducted at stresses below failure, typically exhibit both non-linearity and hysteresis in the stress–strain curve. In a series of three papers in 1965, Walsh explained this behavior in terms of frictional sliding along the faces of closed cracks. Although well known and widely cited, Walsh's model does not seem to have previously been developed in sufficient detail to be used for quantitative predictions. We revisit and extend his model, by including the effect of the stress required to close an initially open crack, and by examining the unloading process in detail. Our analysis leads to closed-form expressions for the loading and unloading portions of the stress–strain curve, as functions of elastic modulus of the uncracked rock, the crack density, the characteristic aspect ratio, and the crack friction coefficient. The model provides a good fit to the loading and unloading portions of the stress–strain curves, for some data on Berea sandstone taken from the literature, and for some new experimental data acquired on thermally cracked La Peyratte granite.

1. Introduction

The mechanical behavior of rocks is to a great extent controlled by the presence of cracks and crack-like voids. This is true both with regards to the elastic behavior of the rock [1], and with regards to inelastic processes such as yielding and failure [2]. In 1965, Walsh [3–5] published a set of three papers that provide the conceptual basis of much of our understanding of the influence of cracks on elastic rock deformation.

Under hydrostatic loading [3], open cracks initially (i.e., at low stresses) contribute an excess compliance to the rock. As the stress is increased, each crack closes up at a stress that is roughly equal to αE, where E is the Young's modulus of the uncracked rock, and α is the initial aspect ratio of the crack. After a crack is closed, it is assumed to make no contribution to the behavior of the rock under hydrostatic loading, because such loading is assumed to cause no resolved shear stress on a closed crack face. This model has been extended [6,7] to account for the presence of a distribution of aspect ratios. The resulting models successfully explain how the bulk compressibility of a cracked rock decreases with increasing confining pressure, eventually leveling off to a value that reflects the intrinsic compressibility of the minerals, along with the influence of any non-closable "equi-dimensional" pores.

Under deviatoric loading, the effect of cracks is more complicated. Consider the case of uniaxial compressive loading, and imagine that there is only one crack, oriented at some angle to the direction of the externally applied axial stress. Initially, the crack is open, and contributes an additional compliance to the rock. At a certain stress, related to the initial aspect ratio and the angle of orientation, the crack will close, causing the effective Young's modulus to increase. Depending on the angle of orientation, a further increase in axial stress may cause the two crack faces to begin to slide. In this situation, the crack contributes to the overall compliance, but by an amount that is different than that of either an open crack or a non-sliding closed crack. If the axial stress is decreased, the cracks will eventually undergo reverse sliding, but in a way that is "asymmetric" with respect to loading and unloading. Hence, the stress–strain curve will exhibit hysteresis. Walsh [4] modeled the cracks as two-dimensional elliptical voids, utilizing the known solution [8] to the elasticity problem for a crack under a compressive stress that is oriented at some arbitrary angle to the crack plane. The constitutive frictional law for closed crack faces was taken to be the classical law of Amontons, in which, during quasi-static sliding, the resolved shear stress τ acting on the closed crack faces must exceed $\mu\sigma$, where σ is the resolved normal stress and μ is the friction coefficient. We follow Walsh's approach, but with a few modifications and extensions. First, Walsh's analysis was a mixture of two- and three-dimensional considerations, in that elasticity solutions for two-dimensional cracks were used, yet the cracks

* Corresponding author. Tel.: +44 207 594 7412; fax: +44 207 594 7444
E-mail address: emmanuel.david08@imperial.ac.uk (E.C. David).

1365-1609/$ - see front matter © 2012 Elsevier Ltd. All rights reserved.
doi:10.1016/j.ijrmms.2012.02.001

were assumed to be three-dimensional objects with their normal vectors distributed randomly in three-dimensional space. Although this has little fundamental influence on the results, the hybrid nature of Walsh's approach renders it difficult to reproduce and extend the model. Hence, we assume a thin plate-like specimen in which all the cracks lie parallel to the "thin" direction, and then consistently use a plane stress analysis. Our results can be converted into those applicable for plane strain by a simple re-definition of the Young's modulus.

More fundamentally, Walsh simplified his calculations by assuming that the stress required to close an initially open crack was negligible compared to the actual applied stress. As the stress required to close a crack increases drastically as the plane of the crack approaches the direction of the externally applied stress, this assumption can never be true for many of the cracks. We eliminate this assumption, and consider both the closure process and the subsequent sliding process. Finally, although Walsh showed that the effective elastic modulus at the onset of unloading will be nearly equal to the modulus of the hypothetical uncracked rock, he did not explicitly analyze the unloading process. We extend the analysis to cover the entire unloading portion of the stress–strain curve.

In the decades following Walsh's original paper, several researchers have developed this model further, in various directions. Kachanov [9] developed a formalism for treating sliding on a system of randomly oriented penny-shaped cracks, including the effects of both an axial stress and a lateral (i.e., traditional triaxial) confining stress, but assumed, as did Walsh, that the crack faces were initially closed. Horii and Nemat-Nasser [10] considered a sliding-crack model based on three-dimensional penny-shaped cracks, but treated in detail only the two limiting cases of $\mu=0$ and $\mu=\infty$. Lawn and Marshall [11] extended Walsh's model by adding a cohesion term to the frictional constitutive law for the cracks, thereby allowing the model to predict yield-type behavior, but again retained the simplification of assuming that the compressive stress required to initially close a crack is negligible. Despite the extensive analysis presented in these and other works, the full implications of Walsh's frictional sliding crack model do not yet seem to have been explicitly developed for the entire "elastic" portion of the loading and unloading process.

We note in passing that a much larger number of papers have been devoted to models in which the cracks propagate under suitably large applied stresses, giving rise to inelastic behavior. The phenomenon of crack extension is outside the intended scope of our model.

2. Effect of a single crack during loading

Consider a rock specimen of length L, width b, and thickness t, containing a single open elliptical crack of half-length c, subjected to a uniaxial compression σ in the longitudinal direction (Fig. 1). The effective Young's modulus of this specimen can be defined by [1]

$$\frac{\sigma^2 bLt}{2E_{\text{eff}}}=\frac{\sigma^2 bLt}{2E}+\Delta W, \tag{1}$$

where E is Young's modulus of the uncracked rock, ΔW is the excess energy stored in the rock due to the presence of the crack, and bLt is the volume of the plate.

If the crack is open, and the plane in which it lies (note: not its normal vector) is oriented at an angle β to the direction of the applied stress, the excess energy term is, under the assumption of plane stress, equal to [4]

$$\Delta W_{\text{open}}=\frac{\pi\sigma^2 c^2 t\sin^2\beta}{E}, \tag{2}$$

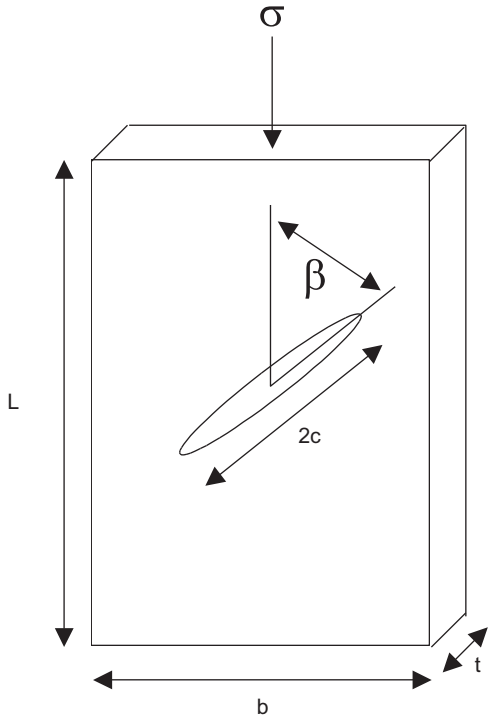

Fig. 1. Thin plate of dimensions $L\times b\times t$, containing a single elliptical crack whose plane makes an angle β with the direction of the applied compressive stress, σ.

This result can be transformed into one appropriate for plane strain by replacing E by $E/(1-\nu^2)$, where ν is the Poisson's ratio of the uncracked rock. To simplify the notation, we consider the case of plane stress, in which case ν does not appear. However, the term $(1-\nu^2)$ is usually very close to unity, in any event. Hence, the effective modulus of a rock containing this single crack will be

$$\frac{E}{E_{\text{eff}}}=1+2\gamma\pi\sin^2\beta, \tag{3}$$

where $\gamma=c^2/bL$ is the two-dimensional crack density parameter.

Now consider the case when the crack is closed, so that the two opposing faces are in contact and sliding past each other. The energy, supplied by the externally applied stress that is required to cause the crack faces to slide is given by [4]

$$\Delta W_{\text{sliding}}=\frac{\pi\sigma c^2 t}{E}(\tau-\tau_f)\sin\beta\cos\beta, \tag{4}$$

where $\sigma\sin\beta\cos\beta=\tau$ is the resolved shear stress along the crack plane, and τ_f is the frictional stress that resists the sliding. Adopting the simplest law of sliding friction, we assume that τ_f will equal $\mu\sigma_n$, where μ is the friction coefficient and σ_n is the resolved normal stress acting on the crack surface. Following Walsh's argument, if σ_c is the normal stress necessary to cause the crack faces to close up and come into contact, then the actual "effective" value of the resolved normal stress acting on the crack will be $\sigma_n^{\text{eff}}=\sigma_n-\sigma_c$. But $\sigma_n=\sigma\sin^2\beta$, so, combining all of these relations, the difference between the resolved shear stress and the frictional resistive shear stress is

$$\tau-\tau_f=\sigma\sin\beta\cos\beta-\mu(\sigma_n-\sigma_c), \tag{5}$$

which is to say,

$$\tau-\tau_f=\sigma\left(\sin\beta\cos\beta-\mu\sin^2\beta+\mu\frac{\sigma_c}{\sigma}\right), \tag{6}$$

Inserting Eq. (6) into Eq. (4) yields

$$\Delta W_{\text{sliding}} = \frac{\pi\sigma^2 c^2 t}{E}\left(\sin\beta\cos\beta - \mu\sin^2\beta + \mu\frac{\sigma_c}{\sigma}\right)\sin\beta\cos\beta, \quad (7)$$

In conjunction with the general expression (1), we can then say that the effective elastic modulus for the rock containing a single sliding crack will be

$$\frac{E}{E_{\text{eff}}} = 1 + 2\gamma\pi(\sin\beta\cos\beta - \mu\sin^2\beta + \mu\frac{\sigma_c}{\sigma})\sin\beta\cos\beta, \quad (8)$$

Finally, we note that if a crack is closed but not sliding, it makes no contribution to the energy, and hence no contribution to the elastic modulus.

2.1. Criterion for a crack to be open or closed

Although we now have relations for the effects on the elastic modulus of an open crack or a closed sliding crack, it remains to derive criteria to decide whether or not a given crack is open or closed, or, if closed, to decide if it is sliding. The normal stress σ_c required to close an elliptical crack whose initial aspect ratio is α is $E\alpha/2$ [12], where α is defined to be the ratio of the minor axis to major axis, so that $\alpha < 1$. Furthermore, by our definition, α is the initial aspect ratio of the crack, at zero stress. The original model of Walsh, as well as the other models mentioned above, correspond to the idealized case of $\alpha = 0$.

The resolved normal stress on the face of the crack is $\sigma_n = \sigma\sin^2\beta$, so the criterion for a crack to be open at an applied compressive stress σ is $\sigma\sin^2\beta < \sigma_c = E\alpha/2$. Hence, at a given stress σ, a crack will be open if $\beta < \beta_c$, and closed if $\beta > \beta_c$, where the critical angle β_c is given by

$$\beta_c(\sigma) = \arcsin\sqrt{\sigma_c/\sigma}. \quad (9)$$

If we normalize the stresses with respect to the stress required to close a crack that is oriented normal to the applied stress, the critical angle can be expressed as

$$\beta_c(\widehat{\sigma}) = \arcsin\sqrt{1/\widehat{\sigma}}, \quad \widehat{\sigma} = \sigma/\sigma_c = 2\sigma/E\alpha. \quad (10)$$

Cracks at all orientations will be open at stresses below σ_c, which is to say, at normalized stresses below 1. When $\widehat{\sigma} = 1$, $\beta_c(\widehat{\sigma}) = \pi/2$, and only those cracks that are precisely normal to the loading direction will close. As σ increases, cracks that are oriented at smaller angles to the loading axis will close, since Eq. (10) shows that the critical angle $\beta_c(\widehat{\sigma})$ decreases as $\widehat{\sigma}$ increases.

2.2. Criterion for a crack to be sliding

For a crack to be sliding, it must of course already be closed. Hence, one necessary condition for sliding is $\beta > \beta_c = \arcsin\sqrt{1/\widehat{\sigma}}$. However, we must also consider the fact that sliding can occur only if the resolved shear stress exceeds the frictional resistive stress, which is to say, from Eq. (6),

$$\sin\beta\cos\beta - \mu\sin^2\beta + \frac{\mu}{\widehat{\sigma}} > 0, \quad (11)$$

Using standard trigonometric identities, this condition can be rearranged as follows:

$$\sin 2\beta + \mu\cos 2\beta - \mu + \frac{2\mu}{\widehat{\sigma}} > 0. \quad (12)$$

$$\cos[2\beta - \arctan(1/\mu)] > \frac{\mu}{\sqrt{1+\mu^2}}\left(1 - \frac{2}{\widehat{\sigma}}\right), \quad (13)$$

which is to say,

$$\beta < \beta_s = \tfrac{1}{2}\left[\arccos\left\{\frac{\mu[1-(2/\widehat{\sigma})]}{\sqrt{1+\mu^2}}\right\} + \arctan\left(\frac{1}{\mu}\right)\right]. \quad (14)$$

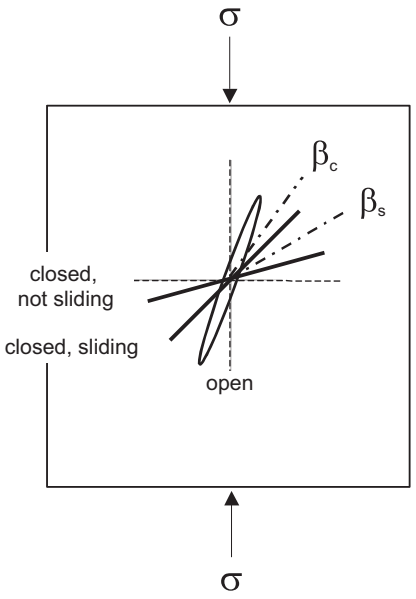

Fig. 2. Three cracks at different orientations, under a given compressive stress, σ. One of the cracks is open, one is closed but not sliding, and the other is closed and sliding. The critical angles that delineate these three regimes are given by Eqs. (10) and (14).

It can be shown by manipulation of Eq. (14) that when $\widehat{\sigma} = 1$, $\beta_s = \pi/2$, and when $\widehat{\sigma} \to \infty$, $\beta_s \to \arctan(1/\mu)$. Moreover, it can be verified numerically that, for all normalized stresses $\widehat{\sigma} > 1$, the critical angle for sliding, β_s, as given by Eq. (14), exceeds the critical angle for closure, β_c, as given by Eq. (10).

To summarize, if $\widehat{\sigma} < 1$, a crack at any orientation to the direction of externally applied stress will be open. If $\widehat{\sigma} > 1$, cracks will be open if $\beta < \beta_c$, and closed if $\beta > \beta_c$, where the critical angle for closure is given by Eq. (10). A closed crack will be sliding if $\beta_c < \beta < \beta_s$, and will not be sliding if $\beta_s < \beta < \pi/2$, where the critical angle for sliding is given by Eq. (14). Since $\beta_c < \beta_s$ for all $\widehat{\sigma} > 1$, there will always be a range of crack orientations for which sliding will occur. The situation is illustrated in Fig. 2.

3. Loading of a rock containing randomly oriented cracks

Now imagine that the rock contains a distribution of N cracks, each with the same size, and with their orientation angles uniformly distributed. By symmetry, we need only consider the range of values $0 \le \beta \le \pi/2$. To simplify the calculations, we invoke the "no-interaction" approximation, in which the excess energy due to each crack is computed as if it were an isolated crack in an infinite body [4,13]. This approximation is very accurate at low crack densities, but becomes increasingly in error as the crack density increases beyond about 0.1 [14]. Alternative methods to approximately account for crack–crack interactions are discussed briefly in Section 6.

In the regime $\widehat{\sigma} < 1$, all cracks are still open. If we continue to ignore interactions between cracks, the contributions of each crack to the compliance will be additive, and so we can average the right-hand side of Eq. (3) over the range $0 \le \beta \le \pi/2$, to find

$$\frac{E}{E_{\text{eff}}} = 1 + \gamma\pi, \quad (15)$$

where $\gamma = Nc^2/bL$ is the standard two-dimensional crack density parameter. If we define a normalized elastic modulus as $\widehat{E} = E_{\text{eff}}/E$, then the normalized modulus for a body containing N randomly distributed open cracks will be $\widehat{E} = 1/(1+\pi\gamma)$.

For $\widehat{\sigma} > 1$, we must integrate the right-hand term in Eq. (3) for those cracks that are open, i.e., $\beta < \beta_c$, and the right-hand side of Eq. (8) for those closed cracks that are sliding, i.e., $\beta_c < \beta < \beta_s$. As mentioned above, cracks for which $\beta > \beta_s$ will be closed and not sliding, and so make no contribution to the energy budget. We now introduce the temporary notation $1/\widehat{E} = 1 + C_{\text{open}} + C_{\text{sliding}}$, where the C terms are compliances due to the open and sliding cracks, respectively.

From Eq. (3), the compliance due to the open cracks, when $\widehat{\sigma} > 1$, is

$$C_{\text{open}} = \frac{2}{\pi}\int_0^{\beta_c} 2\gamma\pi\sin^2\beta\,\mathrm{d}\beta = 4\gamma\left[\frac{\beta}{2} - \frac{1}{4}\sin 2\beta\right]_0^{\arcsin\sqrt{1/\widehat{\sigma}}} = 2\gamma\left(\arcsin\sqrt{1/\widehat{\sigma}} - \frac{1}{\widehat{\sigma}}\sqrt{\widehat{\sigma}-1}\right). \tag{16}$$

Note that γ represents the total crack density; the proportions of cracks that are open or are sliding are accounted for by the stress-dependent limits of integration.

From Eq. (8), the compliance due to the sliding cracks is given by

$$C_{\text{sliding}} = \frac{2}{\pi}\int_{\beta_c}^{\beta_s} 2\gamma\pi(\sin\beta\cos\beta - \mu\sin^2\beta + \mu\frac{1}{\widehat{\sigma}})\sin\beta\cos\beta\,\mathrm{d}\beta = \gamma\left[\tfrac{1}{2}\left(\beta - \frac{\sin 4\beta}{4}\right) - \mu\sin^4\beta - \frac{\mu}{\widehat{\sigma}}\cos 2\beta\right]_{\beta_c}^{\beta_s}, \tag{17}$$

where β_c and β_s are given by Eq. (10) and Eq. (14), respectively. The full expression for the elastic modulus is then given by $1/\widehat{E} = 1 + C_{\text{open}} + C_{\text{sliding}}$.

4. Effect of cracks during unloading

Assume now that the applied compressive axial stress has increased to some value $\sigma^{\max}$, after which it begins to decrease. A decrease in the compressive stress can be thought of as superposition of a tensile stress, i.e., a stress of the opposite sign. If the applied stress is reduced from $\sigma^{\max}$ to some value σ, where $\sigma = \sigma^{\max} - \Delta\sigma$, there will be an associated decrease $\Delta\tau$ in the shear stress acting on the crack, and a decrease $\Delta\tau_f$ in the frictional resistive stress. Reverse sliding will occur if [4]

$$\Delta\tau + \Delta\tau_f - 2\ \tau_f^{\max} > 0, \tag{18}$$

where

$$\Delta\tau = \Delta\sigma\sin\beta\cos\beta = (\sigma^{\max} - \sigma)\sin\beta\cos\beta, \tag{19}$$

$$\Delta\tau_f = \mu\Delta\sigma_n = \mu(\sigma^{\max} - \sigma)\sin^2\beta, \tag{20}$$

$$\tau_f^{\max} = \mu(\sigma_n^{\max} - \sigma_c) = \mu(\sigma^{\max}\sin^2\beta - \sigma_c). \tag{21}$$

Condition (18) for reverse sliding becomes, in terms of the normalized stresses,

$$(\hat{\sigma}^{\max} - \hat{\sigma})\sin\beta\cos\beta + \mu(\hat{\sigma}^{\max} - \hat{\sigma})\sin^2\beta - 2\mu(\hat{\sigma}^{\max}\sin^2\beta - 1) > 0, \tag{22}$$

After some trigonometric manipulation, we find that reverse sliding will occur if the stress during unloading satisfies the following criterion:

$$\mu(\widehat{\sigma}^{\max} + \widehat{\sigma})\cos 2\beta + (\widehat{\sigma}^{\max} - \widehat{\sigma})\sin 2\beta > \mu(\widehat{\sigma}^{\max} + \widehat{\sigma}) - 4\mu, \tag{23}$$

Therefore, the condition for reverse sliding can be summarized as follows:

$$\widehat{\sigma} > 1, \quad \beta_c < \beta < \beta_{\text{rs}}, \tag{24}$$

where the critical (maximum) angle for reverse sliding is given by

$$\beta_{\text{rs}} = \tfrac{1}{2}\left\{\arccos\left[\frac{\mu(\widehat{\sigma}^{\max} + \widehat{\sigma}) - 4\mu}{\sqrt{(\widehat{\sigma}^{\max} - \widehat{\sigma})^2 + \mu^2(\widehat{\sigma}^{\max} + \widehat{\sigma})^2}}\right] + \arctan\left(\frac{\widehat{\sigma}^{\max} - \widehat{\sigma}}{\mu(\widehat{\sigma}^{\max} + \widehat{\sigma})}\right)\right\}. \tag{25}$$

By analogy with Eqs. (4) and (17), and making use of Eqs. (19)–(21), the excess compliance contributed by those cracks that are undergoing reverse sliding will be given by

$$C_{\text{reverse}} = \frac{2}{\pi}\int_{\beta_c}^{\beta_{\text{rs}}} 2\gamma\pi(\Delta\tau + \Delta\tau_f - 2\tau^{\max}{}_f)\sin\beta\cos\beta\,\mathrm{d}\beta = \gamma\left[\tfrac{1}{2}\left(\beta - \frac{\sin 4\beta}{4}\right)\left(\frac{\widehat{\sigma}^{\max}}{\widehat{\sigma}} - 1\right) - \mu(\hat{\sigma}^{\max} + 1)\sin^4\beta - \frac{2\mu}{\widehat{\sigma}}\cos 2\beta\right]_{\beta_c}^{\beta_{\text{rs}}} \tag{26}$$

The full expression for the elastic modulus is now given by $1/\widehat{E} = 1 + C_{\text{open}} + C_{\text{reverse}}$, with C_{open} given by Eq. (16), and C_{reverse} given by Eq. (26).

In order to initiate reverse sliding, Eq. (18) shows that the resolved shear stress must not only start to decrease, but must decrease by a finite amount. Hence, at the onset of unloading, any cracks that had not yet closed during loading will remain open, those closed cracks that had not been sliding remain "stuck", but those cracks that had been sliding will now also be stuck. Hence, the elastic modulus increases by a finite amount at the start of unloading, and so the rock will unload at a steeper slope (when plotted as stress vs. strain) than it had at the end of the loading phase. This model therefore is capable of predicting the existence of hysteresis, as is typically observed in real uniaxial stress–strain curves [15,16,17].

Fig. 3 represents the evolution, as a function of the normalized stress, of the critical angles for closure, sliding and reverse sliding, as given by Eqs. (10), (14) and (25), respectively. The values of these critical angles are not given for $\widehat{\sigma} < 1$, since $\widehat{\sigma} = 1$ is the stress required to close the first crack. The friction coefficient has been taken to be $\mu = 0.6$. The cracks whose orientation is below

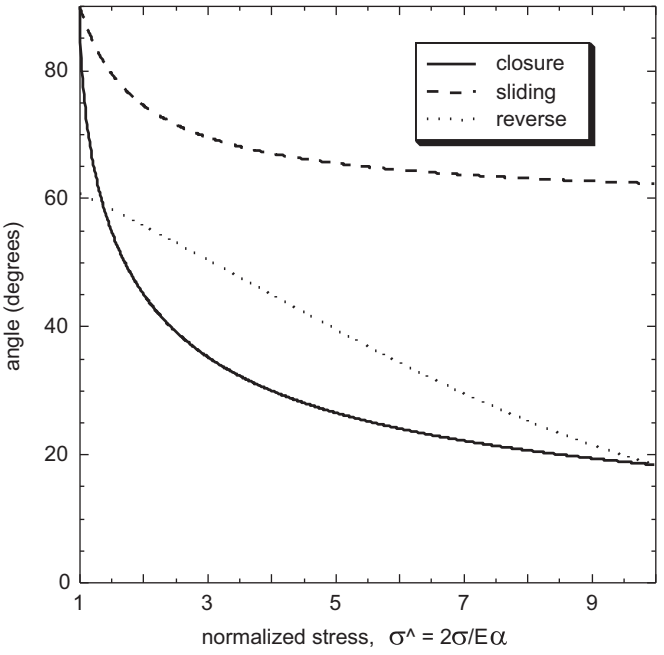

Fig. 3. Evolution, with stress, of the critical angles (in degrees): for closure/opening of the cracks during loading/unloading, as given by Eq. (10); for frictional sliding of the cracks during loading, as given by Eq. (14); and for reverse sliding during unloading, as given by Eq. (25). The friction coefficient is taken to be $\mu = 0.6$.

the closure criteria can be seen as open cracks. Closure proceeds at a rate such that, for example, 70% of the cracks already are closed when $\widehat{\sigma}=4$. Nevertheless, a significant portion of the cracks remain open even for "high" stresses. The cracks mobilized by frictional sliding during loading (or reverse sliding, during unloading) are those cracks lying between the critical angles for closure and sliding (or reverse sliding, during unloading). Note that reverse sliding does not occur at the beginning of unloading; moreover, it can easily be shown from Eq. (25) that as $\widehat{\sigma}\to\widehat{\sigma}^{\max}$, $\beta_{rs}\to\beta_c(\widehat{\sigma}^{\max})=\arcsin\sqrt{1/\widehat{\sigma}^{\max}}$; this result does not depend on the friction coefficient. Fewer cracks are mobilized during unloading than during loading, resulting in hysteresis.

5. Effects of the various parameters

Expressions for the evolution of the elastic modulus with the applied macroscopic stress have been derived, for both the loading and unloading regime. The strain can be calculated by integrating the relation $d\varepsilon=d\sigma/E_{eff}$. From our definitions of normalized stress and modulus, a normalized strain can be defined by $d\widehat{\varepsilon}=d\widehat{\sigma}'/\widehat{E}$. It follows from our previous definitions of $\widehat{\sigma}$ and $\widehat{E}$ that $\widehat{\varepsilon}=2\varepsilon/\alpha$. Except for the regime of $\widehat{\sigma}<1$, when all cracks are still open, the strain must be calculated by numerical integration.

For a given loading–unloading cycle, the normalized modulus and the following normalized stress–strain curve depend on four parameters: the Young's modulus of the uncracked rock, E; the initial aspect ratio of the cracks, α; the crack density, γ; and the friction coefficient acting on the crack faces, μ.

The normalized modulus, $\widehat{E}=E_{eff}/E$, scales inversely with the modulus of the uncracked rock, E. Hence, the dependence on E is trivial.

The aspect ratio enters the model through the definition of the dimensionless stress, $\widehat{\sigma}=2\sigma/E\alpha$. Since $\widehat{E}$ is independent of stress for $\widehat{\sigma}<1$, the aspect ratio controls the stress level at which nonlinear behavior begins. For example, for a hypothetical rock in which $E=20$ GPa and $\alpha=10^{-4}$, nonlinearity (i.e., crack closure and subsequently frictional sliding) begins at a stress of $\sigma=1$ MPa. If the aspect ratio were ten times greater, $\alpha=10^{-3}$, then nonlinearity would begin at $\sigma=10$ MPa.

Fig. 4 shows the stress dependence of the effective modulus, and the resulting stress–strain curves, for three values of the crack density, $\gamma=0.25$, 0.5 and 0.75, for one fixed value of the

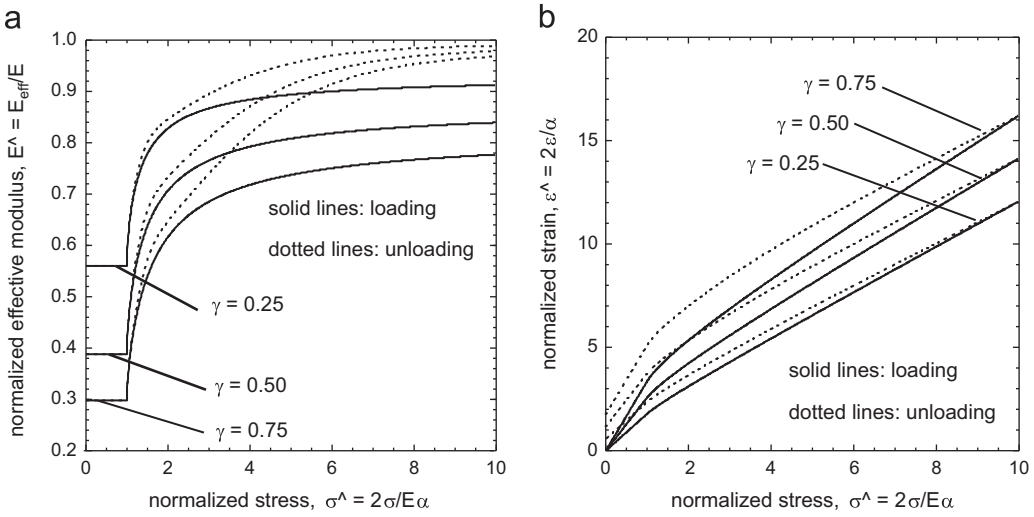

Fig. 4. (a) Normalized effective Young's modulus, and (b) normalized strain, as functions of normalized stress, for a friction coefficient of 0.6, and three values of the crack density: 0.25, 0.5, and 0.75. Solid lines are for loading, dotted lines are for unloading.

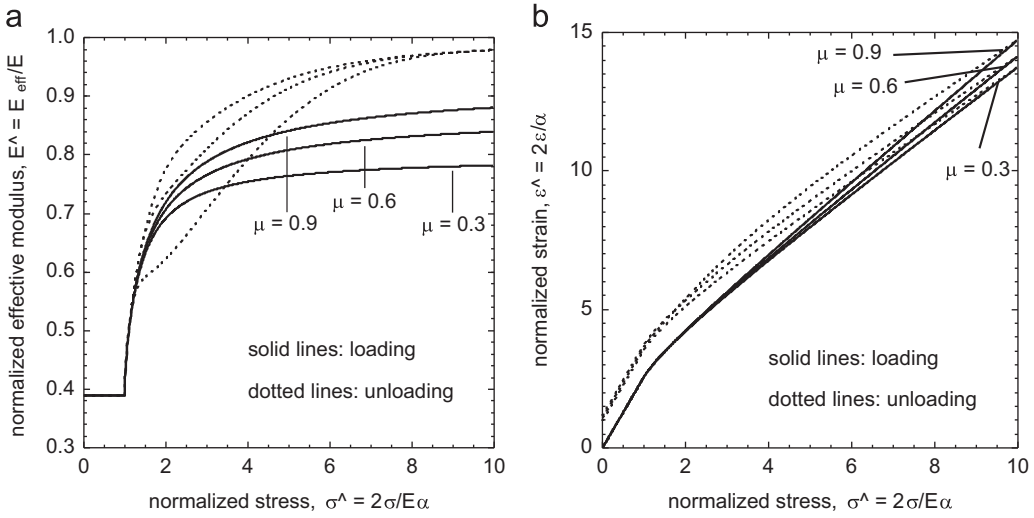

Fig. 5. (a) Normalized effective Young's modulus, and (b) normalized strain, as functions of normalized stress, for a crack density of 0.5, and three values of the friction coefficient: 0.3, 0.6, and 0.9. Solid lines are for loading, dotted lines are for unloading.

friction coefficient, $\mu=0.6$. Fig. 5 shows the equivalent plots for three values of the friction coefficient, $\mu=0.3$, $\mu=0.6$, and $\mu=0.9$, for one fixed value of the crack density, $\gamma=0.5$.

Because we used the no-interaction approximation for calculating the effective modulus, the compliance $(1/\widehat{E})$ is a linear function of crack density. Hence, if all other parameters are held constant, the compliance will be a linear function of γ, although this simple behavior is masked if the modulus is plotted instead of the compliance. The resulting effect of increasing the crack density is a more pronounced compliance, more non-linearity and a larger hysteresis loop, as illustrated in Fig. 4.

The only parameter whose influence cannot be seen in a clear manner from the equations is the friction coefficient, μ. Physically, one can expect the effect of sliding to decrease with increasing values of μ, thus resulting in increasing stiffness, and less pronounced non-linearity and hysteresis, as illustrated in Fig. 5. The extreme case of $\mu=\infty$, although not physically realistic, is not shown in Fig. 5, but would result in a perfectly "reversible" stress–strain curve, without any hysteresis.

It is commonly asserted in the literature that after a phase of non-linearity, caused by the closure of the cracks, the subsequent nearly-linear regime is representative of the compression of an uncracked elastic body. This is a good approximation under hydrostatic stress [7], but not under deviatoric loading. For realistic values of the friction coefficient, as shown in Figs. 4 and 5, frictional sliding of the cracks provides an excess compliance and causes non-linear behavior, although the nonlinearity is less pronounced than that due to the closure of the cracks. For high values of stress, even when the cracks are mainly closed, the effective modulus during loading is never equal to the uncracked modulus, and has a value of usually around 70–90% of E (see Fig. 4(a) and Fig. 5(a)). The uncracked rock modulus E can be only inferred from the slope of the stress–strain curve at the beginning of unloading, as this slope does not depend on any of the microstructural parameters, as the cracks are closed and stuck.

6. Application of model to experimental data

6.1. Berea sandstone

Consider the uniaxial stress–strain curves measured by Guyer et al. [16] and Nihei et al. [17]. In both cases we ignore all data below 4 MPa, as it is well known [18] that in unconfined compression tests, frictional effects between the rock specimen and the loading platen can lead to experimental artifacts in the stress–strain curve that can be quite pronounced in the low stress range. Bésuelle [18] discussed these experimental issues in detail, and made great efforts to avoid these frictional artifacts. More discussion of this assumption is given in Section 6.2.

We used a nonlinear least-squares method to fit our model to these two sets of data, with E, α, γ and μ as the fitting parameters. The residuals tend to have broad minima over quite large regions of the parameter space. However, the precise values of the fitted parameters are of less interest to us than the question of whether or not the entire hysteretic curve can be fit using reasonable values of the parameters. The only parameter that can be inverted with little uncertainty is the aspect ratio of the cracks, α, which controls the stress level at which non-linear behavior begins. There is a partial trade-off between the uncracked modulus E and the crack density γ, with the effect of a higher uncracked modulus being to some extent compensated by a higher crack density, as shown by Eq. (15). However, this trade-off is valid only for low stresses, as non-linearity and hysteresis at higher stresses does not depend on the uncracked modulus. Finally, the friction coefficient, μ, is not very well constrained by the data, since the influence of this parameter is weak, as shown in Fig. 5.

Fig. 6 shows the best fit of the data of Guyer et al. [16], with $E=34\pm1$ GPa, $\alpha=1.9\times10^{-4}\pm10^{-5}$, $\gamma=1.9\pm0.2$, and $\mu=0.75\pm0.1$; the standard deviation is $\sigma_d=3.4\times10^{-5}$. The best fit to the data of Nihei et al. [17]; is shown in Fig. 7, with $E=27\pm1$ GPa, $\alpha=1.9\times10^{-4}\pm10^{-5}$, $\gamma=1.5\pm0.2$, and $\mu=0.75\pm0.1$; the standard deviation is $\sigma_d=3.0\times10^{-5}$. Our model is able to fit all features of the stress–strain curves, using reasonable value of the parameters.

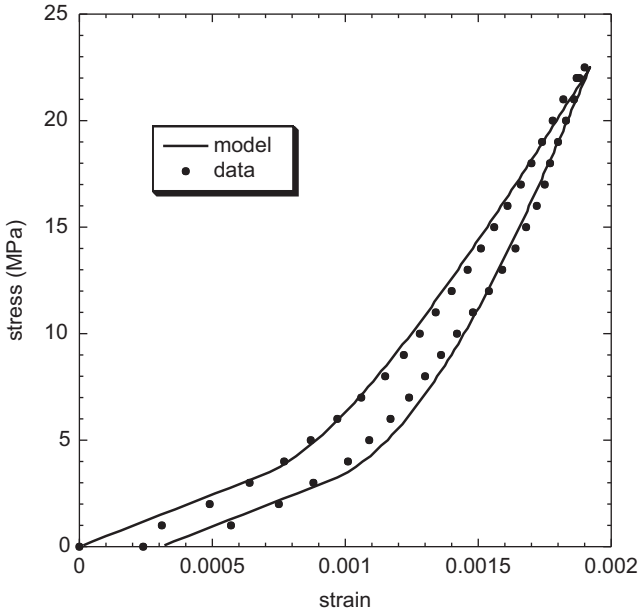

Fig. 6. Uniaxial stress–strain curve of Berea sandstone. Dots are data points from [16], and the curve is generated by our sliding-crack model. Parameter values used in the fits are discussed in the text.

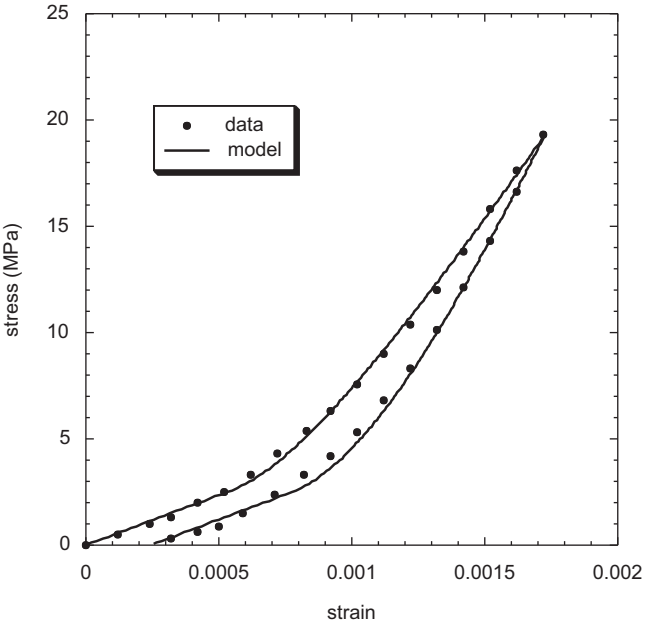

Fig. 7. Uniaxial stress–strain curve of Berea sandstone. Dots are data points from [17], and the curve is generated by our sliding-crack model. Parameter values used in the fits are discussed in the text.

6.2. Thermally cracked granite

We have also carried out a set of uniaxial compression experiments on a thermically cracked granite, at the Laboratoire de Géologie of École Normale Supérieure (Paris). The rock selected was a fine-grained granite from the La Peyratte quarry (France), composed of 40% plagioclase, 26% K-feldspar, 24% quartz and 10% biotite, with a grain size almost constant of around 1.5 mm [19]. The rock has a P-wave velocity anisotropy lower than 1.5%, and so we can consider that the specimens are isotropic. Six cylindrical specimens of 85 mm length and 40 mm diameter were cored and rectified to ensure perfect parallelism of the two end surfaces. One specimen was not thermically treated, and the five other specimens were heat-treated for 24 h at selected temperatures: 200 °C, 300 °C, 400 °C, 500 °C and 600 °C, after which they were directly cooled down to room temperature (RT); such a procedure is known to induce thermal cracking [20,21].

The specimens being previously air dried at 50 °C for 48 h, six uniaxial compression experiments we conducted in dry conditions, realizing a loading–unloading cycle until a constant maximal stress equal to 75 MPa (accuracy of 0.01 MPa). Axial strain measurements were measured using a strain gauge (TML FLA-10–11, Tokyosokki) glued onto the specimen's surface (accuracy of 10^{-6}). The strain rate was $\sim 2\times 10^{-6}$/s. Following Bésuelle [18], frictional effects were reduced in our experimental tests by using a lubricant (50% Vaseline and 50% stearic acid). We then removed a small amount of stress (of around 4 MPa) from the data, corresponding to what we considered to reflect frictional effects. The corresponding strain that was removed, of around 10^{-4}, is very small compared to the total strain eventually undergone by the specimen (see Fig. 8).

The maximal axial stress chosen (75 MPa), which was constant in all six tests, is approximately 30% of the UCS of the rock, whose measured value is between 210 MPa and 230 MPa. An acoustic transducer glued to the surface of the specimen revealed no acoustic emissions throughout the loading–unloading cycle, confirming the absence of crack extension, which is an additional argument to confirm that all the uniaxial tests were conducted in the purely "elastic" regime. Note that the maximum stresses in Fig. 8 are each less than 75 MPa, due to the aforementioned removal of the suspect low-stress data, the precise range of which differed slightly in each case.

Thermal cracking is known to cause the formation of many cracks in a rock [20,21,22]. We then expect the aspect ratio of the cracks, as well as the crack density, to vary between the specimens; on the other hand, there is no a priori reason for the modulus of the "uncracked" rock and the friction coefficient to be changed with thermal cracking. So, we performed a full inversion of the six experimental stress–strain curves, assuming that E and μ are the same for all the specimens, allowing only α and γ to vary between the six heat-treated specimens.

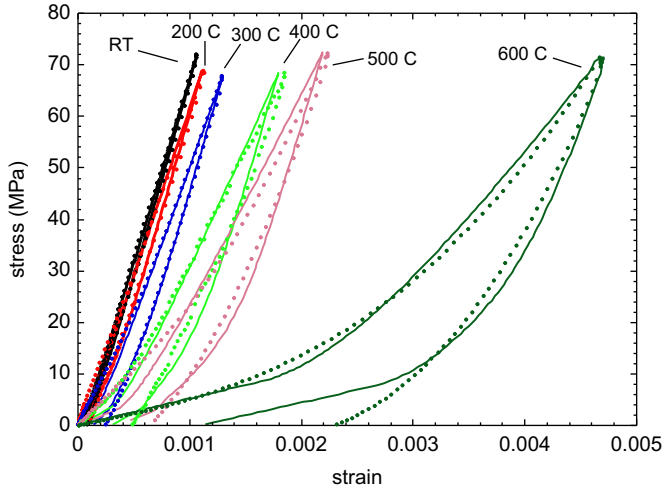

Fig. 8. Uniaxial stress–strain curves for six thermically treated specimens of La Peyratte granite. The dots represent the measured values, and the curves are generated by our sliding-crack model. Parameter values used in the fits are discussed in the text.

By least-square inversion, the best fit of the data is obtained using $E=74\pm 1$ GPa and $\mu=0.60\pm 0.05$ for all the cracked specimens (Fig. 8). The aspect ratios and crack densities obtained from the inversions, which vary for each specimen, are shown in Table 1. Considering the highly nonlinear and hysteretic shape of the stress–strain curve, it can be said that the model does a good job of capturing its essential features. Moreover, the values of the parameters used in this fit are all reasonable. As might be expected, the most notable change in any of the fitting parameters occurred in the crack density, which, according to our model, increased from 0.2 to 4.4 upon heat treatment. Indeed, differences of thermal expansion between the minerals cause crack nucleation; in particular, the drastic increase of crack density between 500 °C and 600 °C is known to be due to the α–β transition of quartz, which occurs at 576 °C [20].

Previous uniaxial compression tests on La Peyratte granite reported the value $E=75$ GPa [21], which is consistent with the value we found, $E=74$ GPa. Note that E in this context represents the modulus of the "uncracked" rock, which reflects the influence of any non-closable, equi-dimensional pores. Hence, it should be less than the mean modulus E_0 of the minerals that comprise the rock [7]. For the case of the 600 °C specimen, we observe a total deformation of around 0.5%. According to our model, a stress of around 8 MPa, easily calculated from Eq. (10), is required to close the first cracks. The maximal stress of 75 MPa in the experiment is ten times greater than this, which shows that most of the cracks should have been closed (see Fig. 3). Hence, roughly speaking, the total deformation of 0.5% must then represent the "compliant" crack porosity of the rock. Double weight measurements gave a total porosity of 2.4% on this specimen. If we consider the crack porosity to be about 0.5%, the equant porosity should be around 2%. The Voigt and Reuss bounds calculated from the mineralogical composition of this granite [23] are 75 GPa and 79 GPa, respectively, giving a Voigt–Reuss average modulus $E_0=77$ GPa for the mineral frame, which is slightly greater than the uncracked rock modulus, which we estimated from the inversions to be 74 GPa. The effect of non-closable pores on the elastic modulus can be approximated by $E/E_0=(1-\phi)^2$ [7]. If we assume that pores are nearly spherical and $E_0=77$ GPa from the Voigt–Reuss average, a non-closable porosity of 2% gives $E=74$ GPa for the uncracked granite, in agreement with the value obtained from our inversion. This is further evidence that the ability of our model to fit the data is not merely fortuitous.

The values of all the fitted parameters are plausible and well constrained; however, very high crack densities such as the best-fitting crack density of 4.4 for the 600 °C specimen might appear difficult to accept. Such a high crack density is to some extent an artifact of having neglected stress-field interactions between nearby cracks. If we had utilized the differential effective medium theory (DEMT; [13,24]) instead of the no-interaction approximation (NI), for example, then the effective modulus in the case of open cracks, as given by Eq. (15), would be replaced by $\widehat{E}=\exp(-\pi\gamma)$. This is equivalent to re-scaling the crack density according to $\gamma_{\mathrm{demt}}=(1/\pi)\ln(1+\pi\gamma_{\mathrm{ni}})$. Assuming that this same scaling relationship would hold for the closed cracks, then the crack density inferred from the data for the granite treated at 600 °C would be only 0.86, instead of 4.4. For the untreated specimen (RT), the differential effective medium theory would give a crack density of 0.16, instead of 0.2. Because all effective

Table 1
The aspect ratios, crack densities and standard deviations (of the strain), as obtained from the least-squares inversions, as functions of the temperature at which the specimens were heat-treated.

T	RT	200 °C	300 °C	400 °C	500 °C	600 °C
$\alpha(\pm 10^{-5})$	1.1×10^{-4}	5×10^{-5}	8×10^{-5}	8×10^{-5}	8×10^{-5}	2.1×10^{-4}
$\gamma(\pm 0.1)$	0.2	0.4	0.7	1.6	2.2	4.4
σ_d	1.7×10^{-5}	2.4×10^{-5}	3.9×10^{-5}	5.8×10^{-5}	9.8×10^{-5}	3.03×10^{-4}

medium theories that attempt to account for crack–crack interactions predict an enhanced effect of crack density on the elastic moduli, using any of these other theories in place of the no-interaction theory would lead to smaller, and presumably more realistic, values of the crack density. However, the contentious question of which effective medium theory best accounts for interactions between cracks is beyond the scope of our present work.

7. Conclusions

Walsh's conceptual model for the effect of sliding cracks on the uniaxial loading of a rock in its elastic range has been extended throughout the entire loading and unloading cycle. Expressions have been derived for the energy contributions of open cracks (O), cracks that are closed and sliding (S), and cracks that are closed and not sliding (N). Criteria were derived, in terms of the stress level, the friction coefficient, and the orientation of the cracks with respect to the applied stress, to determine which of these three categories each crack falls into. Finally, closed-form expressions were developed for the evolution of the elastic modulus as a function of the applied stress. The model was able to provide good fits to many sets experimental data on the uniaxial deformation: two data sets taken from the literature on Berea sandstone, and a new set of data on six thermically cracked granite specimens. For this latter set of data, we found that all the stress–strain curves can be inverted from the model assuming that the specimens have the same friction coefficient and uncracked rock modulus, with only the aspect ratio of the cracks and the crack density varying with thermal cracking. Pre-heating of the specimens caused the crack density to increase drastically, particularly for the core that passed through the α–β phase transition of quartz.

This simple model fits well many sets of uniaxial compression data, using only a few microstructural parameters: E, α, γ and μ. We have also developed the model for the case of an exponential distribution of aspect ratios. Although presumably more physically realistic, this model requires much more elaborate calculations, with a negligible influence on the results, and so has not been presented in this paper. There seems to be no need to consider a distribution of aspect ratios, since the uniaxial behavior can be well-explained assuming that all the cracks have the same initial aspect ratio α, which has then to be thought of as a representative value for the population of cracks present in the rock.

The ability of such a model to characterize actual numerical values of the parameters is limited by several assumptions. First, we assumed a plate-like specimen under plane stress conditions, with slit-like cracks passing through the entire thickness of the plate. Rectifying this simplification would pose no major conceptual or computational problems, but would merely require additional integrations over the azimuthal angle. The most serious simplification is the assumption that the stress fields around nearby cracks do not interact with each other. For purely elastic behavior, these interactions can be accounted for by various simple effective medium theories [13], but the applicability of these methods to dissipative processes such as crack sliding is unclear. Consequently, although we have argued that the inverted crack densities and aspect ratios are realistic, these inverted parameter values should only be considered indicative, in light of the various approximations and simplifications used in the model. We interpret the ability of our model to fit the laboratory data as showing that the qualitative features of the uniaxial stress–strain curve of a rock can indeed be explained in terms of the mechanisms of crack closure and frictional sliding.

One weakness of the model is that the residual strain at the end of unloading is sometimes underestimated (Fig. 8). This implies that the model as developed here might not be applicable to a second, and subsequent, loading–unloading cycles. In any event, extension of our approach to subsequent loading cycles would require all of the criteria for sliding, reverse sliding, etc., to be reconsidered in terms of cracks which have slid and not reverse-slid, cracks which have slid and have reverse-slid, etc.

Our model was developed for conditions of uniaxial compression. In principle, our conceptual model could be extended to the case of triaxial compression, although it is unlikely that the required calculations could be carried through in closed-form.

Acknowledgements

The authors thank Jérôme Fortin (ENS, Paris) for assisting them with the laboratory experiments, and Yves Guéguen (ENS, Paris) for a number of useful comments. They also thank the two IJRMMS reviewers for their critical but constructive comments.

References

[1] Jaeger JC, Cook NGW, Zimmerman RW. Fundamentals of Rock Mechanics. 4th edn. Oxford: Wiley-Blackwell; 2007.
[2] Paterson MS, Wong TF. Experimental Rock Deformation – the Brittle Field.2nd edn. Berlin: Springer; 2005.
[3] Walsh JB. The effect of cracks on the compressibility of rocks. J. Geophys. Res. 1965;70:381–9.
[4] Walsh JB. The effect of cracks on the uniaxial compression of rock. J. Geophys. Res. 1965;70:399–411.
[5] Walsh JB. The effect of cracks in rocks on Poisson's ratio. J. Geophys. Res. 1965;70:5249–57.
[6] Morlier P. Description de l'etát de fissuration d'une roche à partir d'essais non-destructifs simples (Description of the state of fracturization of a rock through simple non-destructive tests). Rock Mech. 1971;3:125–38.
[7] Zimmerman RW. Compressibility of Sandstones. Amsterdam: Elsevier; 1991.
[8] Stevenson AC. Complex potentials in two-dimensional elasticity. Proc. R. Soc. London 1945;184:129–79.
[9] Kachanov ML. A microcrack model of rock inelasticity. Part I: Frictional sliding on microcracks. Mech. Mater. 1982;1:19–27.
[10] Horii H, Nemat-Nasser S. Overall moduli of solids with microcracks: load-induced anisotropy. J. Mech. Phys. Solids 1983;31:155–71.
[11] Lawn BR, Marshall DB. Nonlinear stress–strain curves for solids containing closed cracks with friction. J. Mech. Phys. Solids 1998;46:85–113.
[12] Sneddon IN. The distribution of stresses in the neighbourhood of a crack in an elastic solid. Proc. R. Soc. London 1946;187:229–60.
[13] Zimmerman RW. Effect of microcracks on the elastic moduli of brittle solids. J. Mater. Sci. Lett. 1985;4:1457–60.
[14] Saenger EH, Krüger OS, Shapiro SA. Effective elastic properties of randomly fractured soils: 3D numerical experiments. Geophys. Prospect. 2004;52: 183–95.
[15] Morgenstern NR, Tamuly Phukan AL. Non-linear stress strain relations for a homogeneous sandstone. Int. J. Rock Mech. Min. Sci. 1969;6:127–42.

[16] Guyer RA, McCall KR, Boitnott GN, Hilbert LB, Plona TJ. Quantitative implementation of Preisach–Mayergoyz space to find static and dynamic elastic moduli in rock. J. Geophys. Res. B 1997;103:5281–93.
[17] Nihei KT, Hilbert LB, Cook NGW, Nakagawa S, Myer LR. Frictional effects on the volumetric strain of sandstones. Int. J. Rock Mech. Min. Sci. 2000;37:121–32.
[18] Bésuelle P. 1999. Deformation and rupture in soft rocks and indurate solids: homogeneous behavior and localization. PhD Thesis, University Joseph-Fourier, Grenoble.
[19] Turpault MP. Etude des mécanismes des Altérations Hydrothermales dans les Granites Fracturés (Study of the mechanisms of hydrothermal alteration in fractured granites), PhD Thesis, Univ Poitiers, 1989.
[20] Darot M, Guéguen Y, Baratin ML. Permeability of thermically cracked granite. Geophys. Res. Lett. 1992;19:869–72.
[21] Reuschle T, Gbaguidi Haore S, Darot M. Microstructural control on the elastic properties of thermally cracked granite. Tectonophysics 2003;370:95–104.
[22] Nasseri MHB, Schubnel A, Young RP. Coupled evolutions of fracture toughness and elastic wave velocities at high crack density in thermally treated Westerly granite. Int. J. Rock Mech. Min. Sci. 2007;44:601–16.
[23] Landolt H, Bornstein R. Physical Properties of Rocks, 1a. Berlin: Springer; 1982.
[24] Hashin Z. The differential scheme and its applications to cracked materials. J. Mech. Phys. Solids 1988;36:719–34.